Chapter 11

3-D GEOMETRIC MORPHOMETRIC ANALYSIS OF THE SCLADINA NEANDERTAL CHILD'S MANDIBLE IN A DEVELOPMENTAL CONTEXT

Katerina HARVATI & Michel TOUSSAINT

Michel Toussaint & Dominique Bonjean (eds.), 2014.
The Scladina I-4A Juvenile Neandertal (Andenne, Belgium),
Palaeoanthropology and Context
Études et Recherches Archéologiques de l'Université de Liège, 134: 215-222.

1. Introduction

The Scladina specimen represents a subadult individual of an Early Neandertal, dated to the OIS 5. Age at death is estimated at close to 8 years (Toussaint & Pirson 2006; Smith et al., 2007 & Chapter 8). Morphology, both metric and non-metric, closely aligns the child with Neandertals, as does the mtDNA sequences recovered from the specimen (Orlando et al., 2006). In this study we analyze the three-dimensional shape of the Scladina I-4A juvenile mandible and place it within a comparative developmental context of both modern human and Neandertal samples.

2. Materials and methods

The fossil sample used in this study comprised seven adult and six subadult Neandertal mandibles. When the original fossil specimens were not available for study, we measured high quality casts from the collections of the Division of Anthropology (American Museum of Natural History, New York), the Department of Human Evolution (Max Planck Institute for Evolutionary Anthropology, Leipzig) and the Institut de Paléontologie Humaine (Paris). We also used a recent human comparative sample of thirty two adult and thirteen subadult South African Khoisan as well as ten adult Greenland and Alaskan Inuit mandibular specimens (Table 1). The subadult specimens, both Neandertal and modern human, were subdivided into six categories based on stage of dental eruption: 1. neonate–2 years old; 2. 2–5 years old; 3. 5–8 years old; 4. 8–10 years old; 5. 10–15 years old; and 6. 15–20 years old. This was done because of the uncertainty inherent in the aging of individuals based on dental eruption stages, and due to the paucity of fossil juvenile remains. The age categories were displayed in the principal component plots by their number (Figure 2). Although the human mandible is sexually dimorphic (Hrdlička, 1940^{a,b}; Humphrey et al., 1999), sexually dimorphic patterns differ regionally in modern humans (Humphrey et al., 1999) and probably also across taxa. In addition, sex assignment is very difficult in subadults.

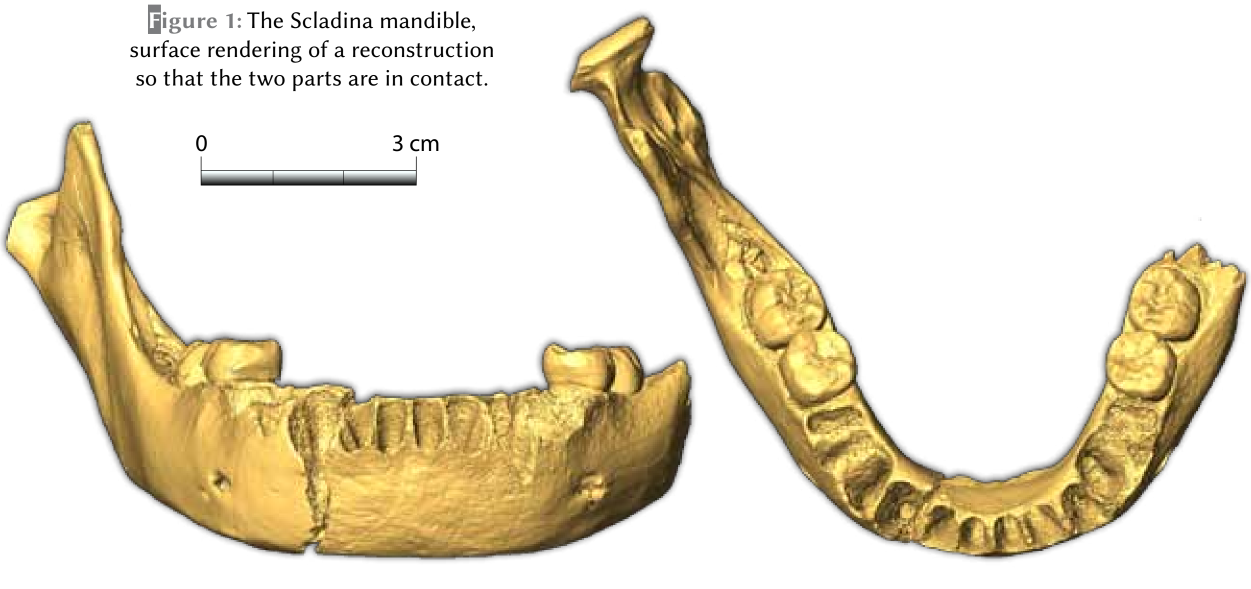

Figure 1: The Scladina mandible, surface rendering of a reconstruction so that the two parts are in contact.

Modern humans	
Khoisan adults	32 (SAM, UCT)
Khoisan subadults	13 (SAM, UCT)
Inuit adults	10 (AMNH)
Fossils	
Neandertal adults (7)	Krapina J, La Ferrassie 1, La Quina 9, Montmaurin, Regourdou, Tabun 1, Zafarraya
Neandertal subadults (6)	Gibraltar 2, Le Moustier, Pech de l'Azé, Roc de Marsal, Scladina I-4A, Teshik-Tash
H. heidelbergensis (2)	Mauer, Sima 5

Table 1: 70 mandibles constitute the basis of this comparative study.

Because no sex information was available for most of our samples, males and females were pooled in the analysis, and sexual dimorphism was not examined in this study.

A surface rendering of the Scladina specimen was measured using the software Amira (Figure 1), while the comparative sample was measured directly with a Microscribe 3D-X (Immersion Corp.) portable digitizer. Fifteen osteometric landmarks, defined as homologous points that can be reliably and repeatedly located and which represented the midline and left side of the mandible were used (Table 2 and Figure 2; see also Nicholson & Harvati, 2006). All data were collected by one observer (KH). This type of morphometric analysis does not accommodate missing data. Therefore some data reconstruction was undertaken. Landmarks on specimens with minimal damage were estimated during data collection, using anatomical clues from the preserved surrounding areas. Bilateral landmarks missing on the left side were estimated from the preserved homologues on the right side by mirroring-imaging, using reflected relabeling (Harvati, 2003). This procedure exploits the Procrustes geometry to reflect the paired landmarks without having to specify a mirroring plane. During reflected relabeling, specimens with a missing landmark on one side were least-squared superimposed with their reflections. The coordinates for the missing landmark were then substituted from the fitted homologous points in the preserved side. The level of error that is introduced by this procedure has been shown to be minimal (Harvati, 2003).

The landmark coordinates were processed according to geometric morphometric methods. Specimen configurations were superimposed using Procrustes Generalized Analysis (GPA) using the Morpheus software package

Landmark	Definition
1. Gonion	The point along the rounded posterioinferior corner of the mandible where the line bisecting the angle between the body and the ramus would meet
2. Posterior ramus	The point at the posterior margin of the ramus at the level of the M_3
3. Condyle tip	The most superior point on the mandibular condyle
4. Condylion mediale	The most medial point on the mandibular condyle
5. Condylion laterale	The most lateral point on the mandibular condyle
6. Root of sigmoid process	The point where the mandibular notch intersects the condyle
7. Mandibular notch	The most inferior point on the mandibular notch
8. Coronion	The most superior point on the coronoid process
9. Anterior ramus	The point at the anterior margin of the ramus at the level of the M_3
10. M_3	The point on the alveolar bone just posterior to the midline of the third molar
11. Mental foramen	The point in the middle of the mental foramen
12. Canine	The point on the alveolar margin between the canine and the first premolar
13. Gnathion	The most inferior midline point on the symphysis
14. Infradentale	The midline point at the superior tip of the septum between the mandibular central incisors
15. Mandibular orale	The most superior midline point on the lingual side of the mandible between the two central incisors

Table 2: Landmarks used and their definitions. The first 12 landmarks were collected on the left side. Adapted from Nicholson & Harvati, 2006.

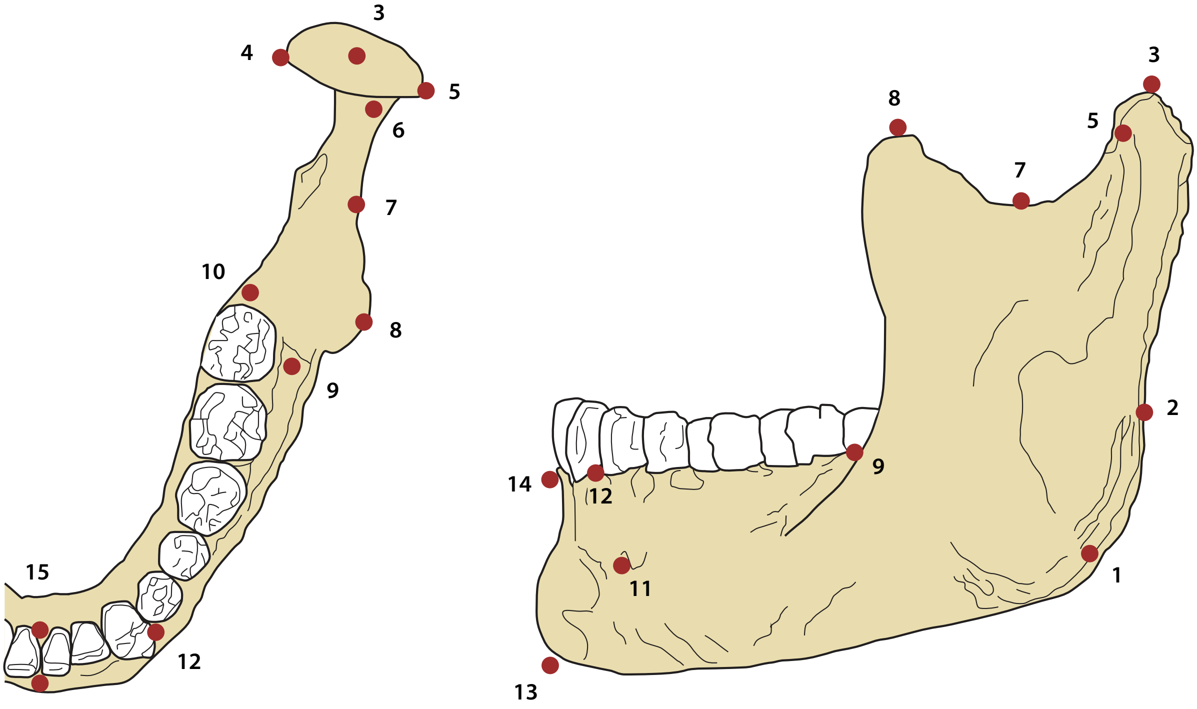

Figure 2: Landmarks used in this analysis (adapted from Nicholson & Harvati, 2006). Landmark numbers correspond to those listed in Table 2.

(Slice, 1998). This procedure translates the landmark configurations to common origin, scales them to unit centroid size (the square root of the sum of squared distances of all landmarks to the centroid of the object, the measure of size used here), and rotates them according to a best-fit criteria. During GPS centroid size is removed.

To explore the relationship of Scladina to the Neandertal and modern human comparative samples, a principal components analysis (PCA) was conducted using the superimposed coordinates as variables (shape space). Additionally, and in order to analyze the growth trajectories of Neandertals and modern humans, we conducted a PCA using the superimposed coordinates and the logarithm of centroid size (logCS) as variables (size-shape space), as outlined by Mitteroecker et al. (2004). In such an analysis of size-shape space, data logCS has the greatest variance of any other variable, and thus the first principal component reflects differences in size and can be interpreted as a temporal pattern of shape change. Higher size-shape principal components in turn can be interpreted as spatial patterning of shape changes reflecting taxonomic differentiation along a growth trajectory. Because biological interpretations can sometimes be affected by the projection of a higher-dimension space onto two dimensions, we examined the first three principal components following Mitteroecker et al. (2004).

The GPS, size-shape principal components analysis, and visualization of shape differences along size-shape principal components were conducted using Morphologika 2 (O'Higgins & Jones, 2006). The three-dimensional plots of principal components 1, 2 and 3 were made using the SAS software package (SAS Institute, 1999-2001).

3. Results

The results of the principal components analyses are shown in Figures 3-6.

Shape-space analysis: Neandertal and modern human adults were separated along principal component 1 (26.1% of the total variance), although there was some overlap along this axis (Figure 3). PC 1 also separated subadults (both modern and Neandertal) from modern human, but not Neandertal adults. PC 2 separated Neandertal and Khoisan adults from modern human and some Neandertal subadults. Inuit adults for the most part overlapped with Khoisan subadults along that axis. Scladina fell with Neandertals on the positive ends of both PC 1 and 2. The two *H. heidelbergensis* specimens clustered with Neandertals, but fell near the zone of overlap with modern humans along PC 1.

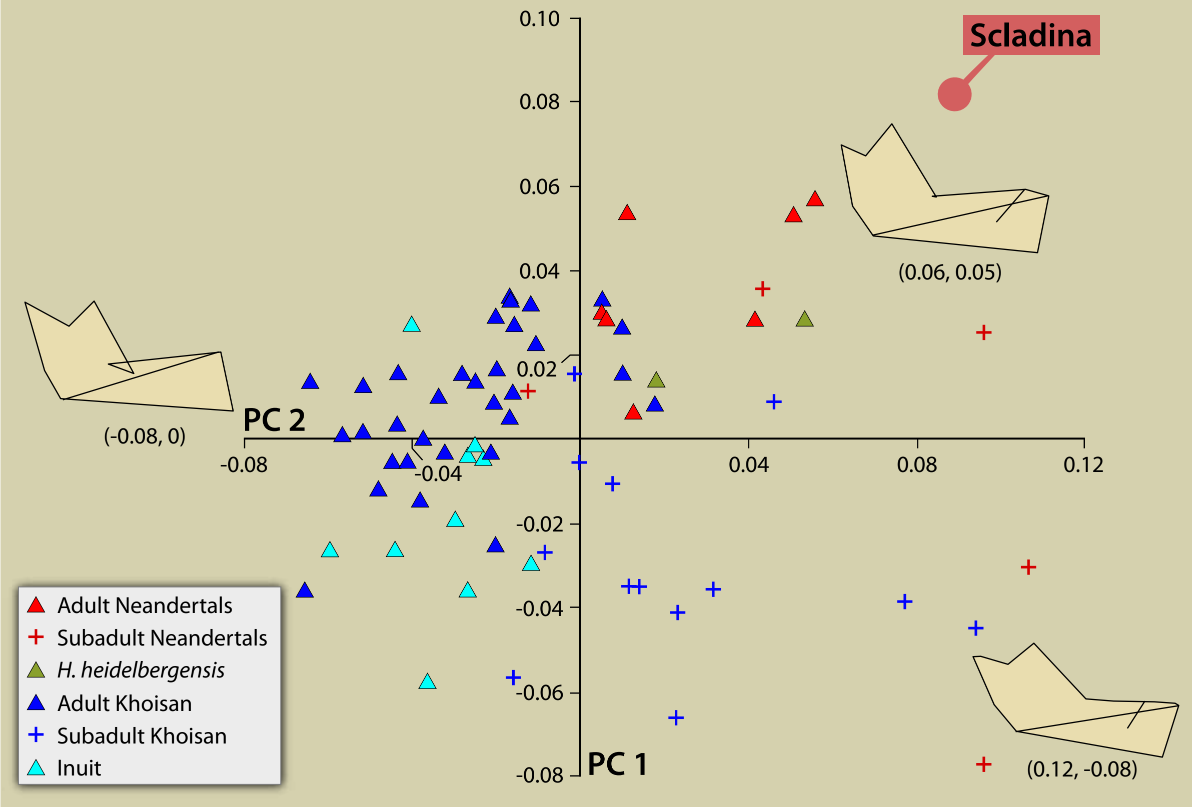

Figure 3: Shape-space analysis. Principal components 1 (x-axis) and 2 (y-axis). Shape differences shown between Neandertals (positive ends of PC1 and 2), juvenile *Homo sapiens* (positive end of PC1, negative end of PC2) and adult *Homo sapiens* (negative end of PC1).

Shape differences along PC 1 included on the Neandertal/subadult (positive) end: a short condyle, an infero-posteriorly inclined symphysis, an anteriorly placed distal end of the toothrow, a medially placed gonion, lateral position of the condyle relative to the mandibular notch, and a posterior and lateral position of the mental foramen. Shape changes along PC 2, on the other hand, included on the juvenile/Inuit (positive) end: a more posteriorly sloping ramus and posterior position of the condyle, short ramus and corpus height (as reflected at the level of the canine), anteriorly placed distal end of the toothrow, and more medial and anterior position of the canine.

PC 1 was weakly correlated with centroid size when the entire sample was considered ($r^2 = 0.07$, $p = 0.04$), but the correlation was much stronger when *Homo sapiens* and *Homo neanderthalensis* were examined separately (Neandertals: $r^2 = 0.56$, $p = 0.003$; *Homo sapiens*: $r^2 = 0.44$, $p < 0.0001$). When plotted against centroid size (Figure 4, left panel), Neandertals, adults and subadults, were clearly more similar in their PC 1 scores to Khoisan subadults but were well separated from modern human adults. While the subadults had a similar starting point, the trajectory of Neandertals with increasing size (and time) along PC1 was very different from that of modern humans. PC 2 was also mildly correlated with centroid size when the entire sample was analyzed either in its entirety ($r^2 = 0.16$, $p = 0.0005$) or separately (Neandertals: $r^2 = 0.29$, $p = 0.06$; *Homo sapiens*: $r^2 = 0.07$, $p < 0.04$). Figure 4 (right panel) also shows Neandertals and modern humans have a similar starting point on PC 2 and this time follow a similar trajectory with increasing size, though the Neandertal trajectory is longer than that of modern humans.

Form-space analysis: The results of the shape-space analysis were confirmed with a form (or size-shape) -space analysis. Here principal component 1 accounted for 78.9% of the total variance (Figure 5) and very closely reflected differences in size (Figure 5). PC 1, therefore, can be interpreted as a temporal axis with younger individuals placed on the negative side and older ones on the positive end of the axis. PC 2 accounted for 5.6% of the total variance and showed spatial patterning. This information can be interpreted as reflecting taxonomic differences between Neandertal and modern human

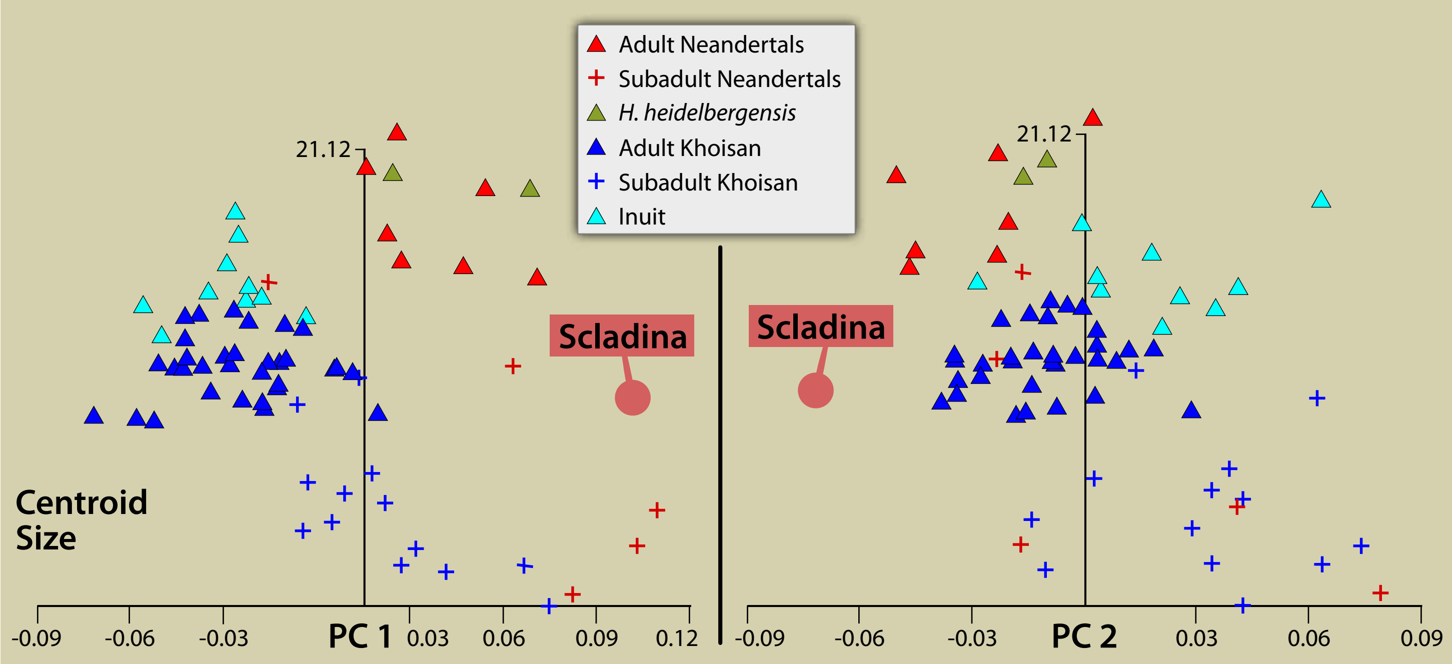

Figure 4: Shape-space analysis. Principal component 1 (left panel) and 2 (right panel) plotted against centroid size.

mandibular shape. Neandertals, both subadults and adults, and *H. heidelbergensis* clustered on the positive side of PC 2, with modern human adults and subadults on the negative side. While there was no overlap among adults, some Neandertal subadults fell at the edge of the modern human range of variation: Le Pech de l'Azé fell very close to a Khoisan child of similar chronological age; the Le Moustier adolescent fell within the range of modern adults on PC 2. Nonetheless, the Scladina individual was well on the positive end of PC 2, at the edge of the adult Neandertal range on that axis (Figure 5).

Although Neandertal and modern human subadults are closer to each other than the adults are, the principal shape differences distinguishing the taxa are already seen in young individuals (age category 2 [2–5 years] being the smallest one included in this analysis). Scladina, at the dental stage 4, is already characterized by the taxonomic features that differentiate Neandertals from modern humans. This finding is consistent with previous results that the anatomical features that distinguish Neandertals from modern humans appear either prenatally or early postnatally (Ponce de León & Zollikofer

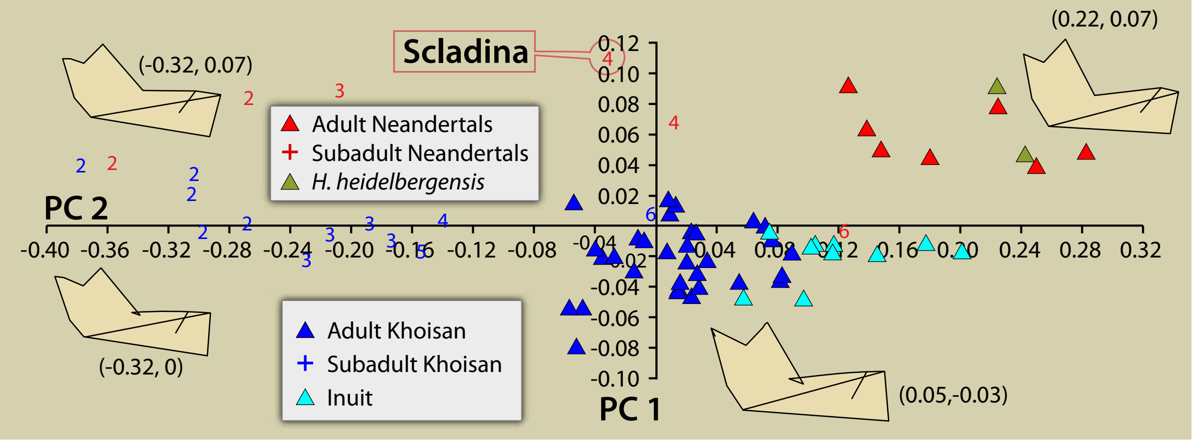

Figure 5: Size-shape space principal components analysis. PC1 (x-axis) plotted against PC 2 (y-axis). Shape differences along PC1 and 2 are shown. Age categories as follows: 1: Neonate–2 years old; 2: 2–5 years old; 3: 5–8 years old; 4: 8–10 years old; 5: 10–15 years old; 6: 15–20 years old.

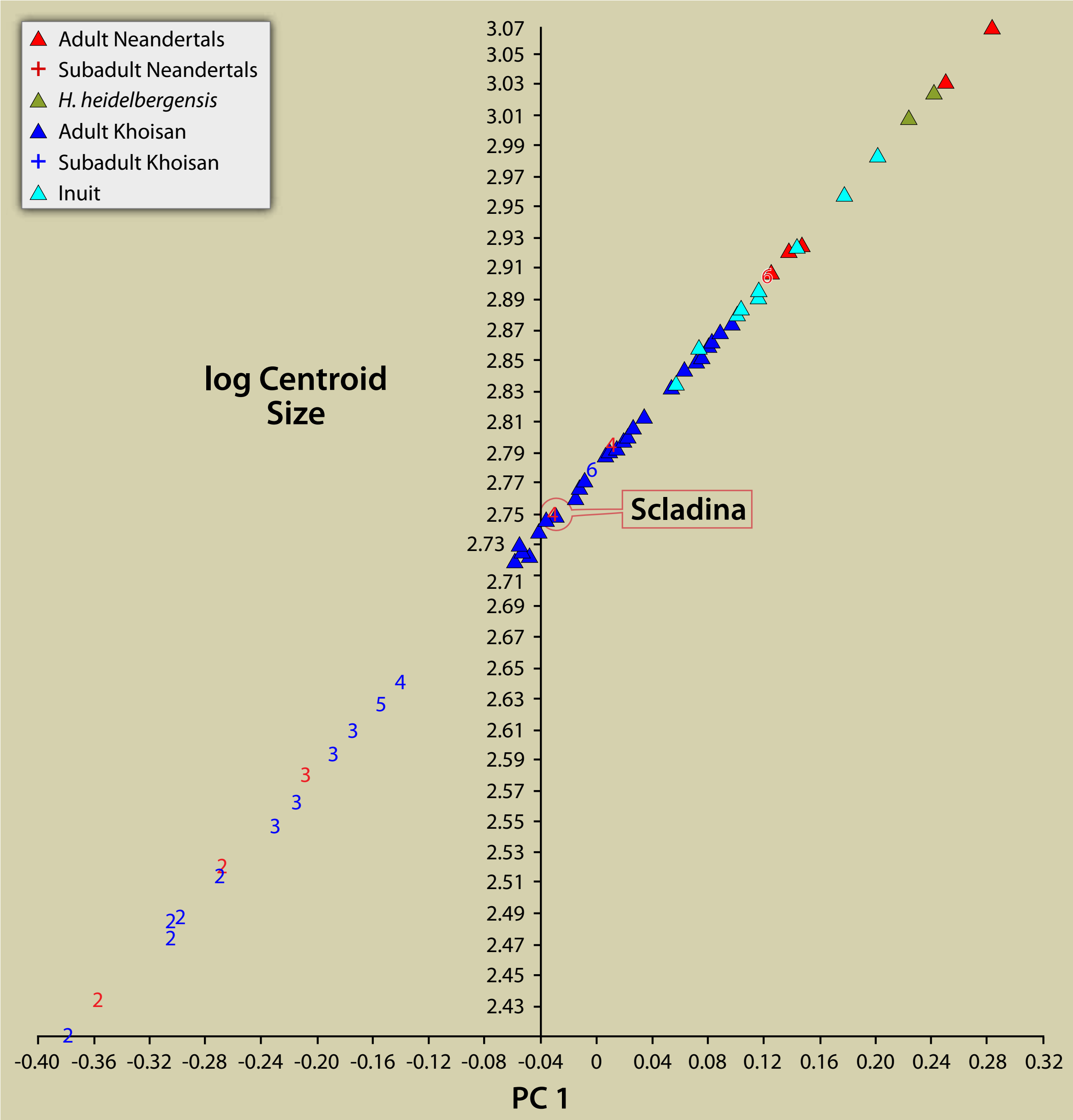

Figure 6: PC 1 plotted against log centroid size. Age categories as follows: 1: Neonate–2 years old; 2: 2–5 years old; 3: 5–8 years old; 4: 8–10 years old; 5: 10–15 years old; 6: 15–20 years old.

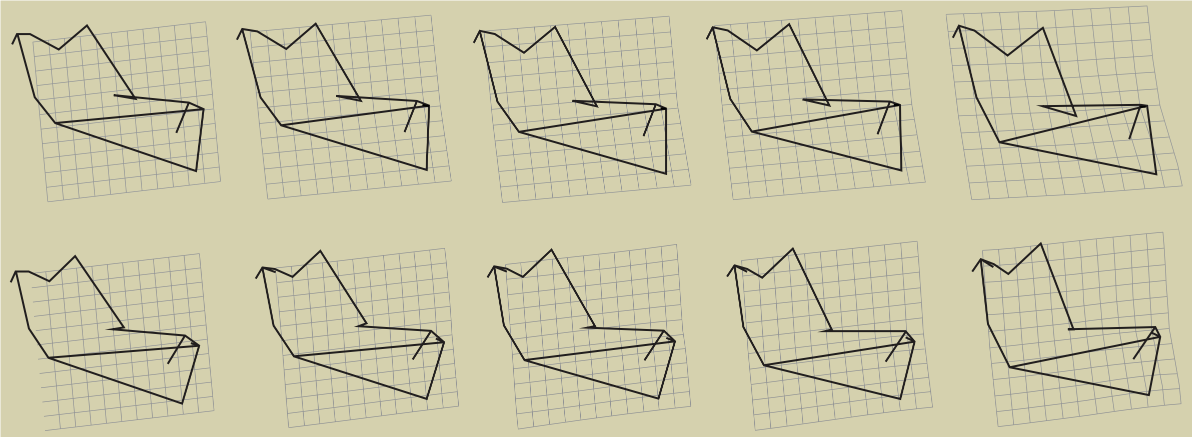

Figure 7: The modern human (above) and Neandertal (below) growth trajectories along PC 1:

2001, 2006; Bastir et al. 2007). The Neandertal growth trajectory is longer along PC 1 and overlaps partially only with some of the larger individuals from the Inuit sample. Neandertal subadults, particularly those in the later stages (4–6), are more advanced along PC 1 than modern human children of similar dental stage (Figure 5). Scladina, with a dental stage of 4, overlaps on PC 1 with modern Khoisan adults, while Le Moustier (dental stage 6) overlaps with some of the larger Inuit adults.

The modern human trajectory along PC 1 (Figure 7) can be described as showing growth in both the vertical and anterior dimension, with an increase in the ramal height, a change in the orientation between the ramus and the body, and an increase in the antero-posterior length of the body being the dominant features. The Neandertal trajectory is similar in the vertical component of growth and is also characterized by a change in the relative position and orientation of the ramus and body, though not by a pronounced antero-posterior direction of growth (Figure 7).

4. Discussion and conclusions

This study shows that the Scladina mandible, although quite young in chronological age and relatively old in geological age, is already characterized by the features that distinguish Neandertals from modern humans as reflected by our data. The data also found that Neandertal juveniles show some of the crucial features differentiating Neandertal from modern human adults at an early age. Nonetheless both groups are characterized by considerable shape change throughout ontogeny. These results are consistent with previous work indicating that both prenatal development and postnatal growth are important in determining the adult Neandertal and modern human mandibular shape (Bastir et al., 2007). The Neandertal growth trajectory was found to be longer than that of modern humans, reaching a larger adult form, though the inclusion of a large-bodied modern human group (Inuit) resulted in more overlap in size than previously reported (Bastir et al., 2007). Neandertal juveniles appeared to be more advanced than modern human juveniles of similar dental stage, though this was more apparent in the later stages of growth.

Acknowledgements

We are grateful to all curators in various institutions in Europe, Africa and Israel for allowing us to study the fossil and recent human collections in their care. We also thank Jean-Jacques Hublin and Philipp Gunz. This is NYCEP morphometric contribution N° 36. Funding for this research was provided by the Max Planck Society, the Wenner-Gren Foundation and the EVAN Marie Curie Research Training Network MRTN-CT-019564.

References

Bastir M., O'Higgins P. & Rosas A. 2007. Facial ontogeny in Neanderthals and modern humans. *Proceedings of the Royal Society B: Biological Sciences*, 274: 1125-1132.

Harvati K., 2003.The Neanderthal taxonomic position: models of intra- and inter-specific craniofacial variation. *Journal of Human evolution*, 44: 107–132.

Hrdlička A., 1940^{a}. Lower jaw. The gonial angle, I. The bigonial breadth, II. *American Journal of Physical Anthropology*, 27: 281-308.

Hrdlička A. 1940^{b}. Lower jaw further studies. *American Journal of Physical Anthropology*, 27: 383-467.

Humphrey L. T., Dean M. C. & Stringer C. B., 1999. Morphological variation in great ape and modern human mandibles. *Journal of Anatomy*, 195: 491-513.

Mitteroecker P., Gunz P., Bernhard M., Schaefer K. & Bookstein F. L., 2004. Comparison of cranial ontogenetic trajectories among great apes and humans. *Journal of Human Evolution*, 46: 679-698.

Nicholson E. & Harvati K., 2006. Quantitative Analysis of Human Mandibular Shape Using 3-D Geometric Morphometrics. *American Journal of Physical Anthropology*, 131: 368-383.

O'Higgins P. & Jones N., 2006. *Tools for statistical shape analysis*. Hull York Medical School. http://www.york.ac.uk/res/fme/resources/software.htm.

Orlando L., Darlu P., Toussaint M., Bonjean D., Otte M. & Hänni C., 2006. Revisiting Neandertal diversity with a 100,000 year old mtDNA sequence. *Current Biology*, 16: R400-R402.

Ponce de León M. S. & Zollikofer C. P. E., 2001. Neanderthal cranial ontogeny and its implications for late hominid diversity. *Nature*, 412: 534-538.

Ponce de León, M. S. & Zollikofer C. P. E., 2006. Neanderthals and modern humans — chimps and bonobos: Similarities and differences in development and evolution. In K. Harvati & T. Harrison (eds.), *Neanderthals Revisited: New Approaches and Perspectives*. Dordrecht, Springer: 89-111.

Slice D. E.,1998. Morpheus *et al.*: software for morphometric research. Revision 01-30-98. Department of Ecology and Evolution, State University of New York, Stony Brook.

Smith T. M., Toussaint M., Reid D. J., Olejniczak A. J. & Hublin J.-J., 2007. Rapid dental development in a Middle Paleolithic Belgian Neanderthal. *Proceedings of the National Academy of Sciences of the United States of America*, 104, 51: 20220-20225.

Toussaint M. & Pirson S., 2006. Neandertal Studies in Belgium: 2000-2005. *Periodicum Biologorum*, 108, 3: 373-387.